A global characterization of gap solitary-wave solutions to a coupled KdV system

A. R. Champneys*, M. D. Groves† & P. D. Woods‡

Abstract

Two coupled KdV equations, depending upon three dimensionless parameters, are investigated for gap solitary-wave solutions. Normal-form analysis of two degenerate Hamiltonian-Hopf bifurcations captures small-amplitude envelope solitary waves. Agreement occurs with numerical continuation to large amplitude, linking solitary waves, kinks, and a 'snaking' transition to infinite periodic cores.

PACS: 47.35.+i 05.45 42.65.T 02.30.Hq 02.60.Lj

Keywords: Coupled Korteweg-de Vries equations, solitary waves, reversible 1 : 1 resonance, normal-form analysis, kinks

1 Introduction

Systems of two coupled Korteweg-de Vries (KdV) equations arise in several contexts, for example as a general model for strongly interacting nonlinear waves, as a model for second-harmonic generation in diffractive optical media and in the theory of near-resonant interaction of planetary waves (see [12, 14, 11] and references therein). In general these coupled KdV equations are non-integrable, yet mathematically the global well-posedness of the initial-value problems can be established (cf. [2]). Solitary-wave solutions of such models, if they exist, are important as they are likely to be attractors (after long times) for a wide range of initial data. This Letter aims to characterize, in terms of all possible system parameters, the existence of gap solitary waves. Here the 'gap' refers to parameter configurations in which neither component KdV equation has continuous spectrum. An equivalent condition, which we will adopt here, is that the system of travelling wave ODEs has a hyperbolic zero equilibrium, that is the eigenvalues of the corresponding linearized system all have non-zero real part.

Linearly coupled KdV equations have appeared in at least three forms in the literature. Gear & Grimshaw [12] derived the system of PDEs

$$u_t + 3u^2 + u_{xx} + pv_{xx} + quv + \frac{r}{2}v^2 = 0, \tag{1}$$

$$v_t + \Delta v + 3v^2 + v_{xx} + \lambda\left(pu_{xx} + ruv + \frac{q}{2}v^2\right) = 0 \tag{2}$$

as a model for strongly interacting internal wave modes, Grimshaw and Malomed [14] suggested the equations

$$u_t - \frac{1}{2}(u^2)_x + u_{xxx} = -\lambda v_x, \tag{3}$$

$$v_t - \Delta v_x - \frac{1}{2}(v^2)_x - \alpha v_{xxx} = -\beta\lambda u_x, \tag{4}$$

*Department of Engineering Mathematics, University of Bristol, Bristol, BS8 1TR, UK (Corresponding author. Email: a.r.champneys@bristol.ac.uk)

†Department of Mathematical Sciences, Loughborough University, Loughborough, LE11 3TU, UK

‡Department of Engineering Mathematics, University of Bristol, Bristol BS8 1TR, UK

and Gottwald *et al* [11] proposed slightly different model, namely

$$u_t + u_{xxx} - 6uu_x = v_x, \tag{5}$$
$$v_t + \delta v_{xxx} + \eta v_x - 6\mu v v_x = \kappa u_x. \tag{6}$$

In fact all three systems are effectively equivalent: systems (3), (4) and (5), (6) are identical up to re-definition of various parameters, and system (1), (2) may be put in the form (3), (4) by a linear change of variables, provided that the coefficients satisfy certain non-degeneracy conditions (private communication from R. Grimshaw). In this Letter we will consider the form (5), (6), whose travelling wave reduced system has a freely varying parameter as the coefficient of a nonlinear term (see below), so that it is therefore well suited to normal-form analysis. Making the travelling wave substitution $u = u(z)$, $v = v(z)$, $z = x - ct$ in equation (5), (6) and integrating once, one obtains the equations

$$\ddot{u} = cu + v + 3u^2, \tag{7}$$
$$\ddot{v} = su + (c - \eta)v + \mu v^2, \tag{8}$$

in which the constant of integration has been set to zero to allow for solitary waves, the scaled variables

$$u = A\hat{u}, \quad v = A^2\hat{v}, \quad \mu = (\delta/3A)\hat{\mu}, \quad c = A\hat{c}, \quad \eta = A(\delta\hat{\eta} + (1-\delta)\hat{c}), \quad z = \sqrt{A}\hat{z}$$

have been introduced and the hats have been dropped for notational simplicity; here $A = \sqrt{|\kappa|/|\delta|}$ and $s = \mathrm{sgn}(\kappa/\delta)$.

This Letter concerns the reduced system (7), (8) of ODEs, homoclinic solutions of which correspond to solitary-wave solutions of the original system (5), (6) of PDEs (in this article the word 'homoclinic' used alone always means 'homoclinic to the zero equilibrium'). It is readily verified that the system of PDEs (5), (6) has a Hamiltonian structure, and in keeping with the general theory given by Benjamin [1, §2], this Hamiltonian structure is inherited by the ODE system (7), (8), which can be written in canonical form with Hamiltonian

$$H_{\mathrm{KdV}} = \frac{s}{2}p_1^2 + \frac{1}{2}p_2^2 - \frac{cs}{2}q_1^2 - sq_1q_2 - \frac{1}{2}(c-\eta)q_2^2 - sq_1^3 - \frac{\mu}{3}q_2^3, \tag{9}$$

where $q_1 = u$, $q_2 = v$, $p_1 = s\dot{u}$, $p_2 = \dot{v}$. The system is also reversible in the usual sense: it is invariant under the transformation $(z, q_1, q_2, p_1, p_2) \mapsto (-z, q_1, q_2, -p_1, -p_2)$.

In earlier papers, the present authors used a variety of analytical and numerical techniques to study solitary-wave solutions of extensions to the so-called *fifth-order KdV equation,* which first appeared in the literature around 30 years ago [19, 20] (see refs. [16, 25] for modern derivations). The extensions take the form of either additional nonlinear terms involving higher derivatives [6] or competing quadratic and cubic nonlinearities [23]. It was previously known that the usual fifth-order KdV equation possesses small-amplitude envelope solitary-wave solutions that are associated with a so-called subcritical *Hamiltonian-Hopf bifurcation* or *reversible 1:1 resonance* in the travelling wave ODEs [13] and are found by normal-form analysis [18]. In this bifurcation scenario four purely imaginary eigenvalues collide in pairs and become complex as a parameter is varied. Depending upon the sign of a certain coefficient in the normal form, the resulting hyperbolic equation has either a pair of small-amplitude reversible homoclinic orbits (the subcritical case) or no small-amplitude homoclinic orbits (the supercritical case). The additional parameters introduced via the extra nonlinear terms give rise to the possibilities of further bifurcation phenomena. In particular, there are two possible cases where the Hamiltonian-Hopf bifurcation switches between super- and subcriticality. One of these cases arises in the steady-state version of the generalised Swift-Hohenberg equation [23] and the other in the theory of interfacial waves [7] (both scenarios are briefly discussed in Section 2 below). In this article we will analyse the above coupled KdV system in a similar fashion.

In Section 2 below we locate the Hamiltonian-Hopf bifurcation points for the system (7), (8) in its parameter space. The appropriate normal form is then introduced and certain significant coefficients are calculated. Two degenerate Hamiltonian-Hopf points are identified at which the bifurcation switches between super- and subcriticality. One of these points falls into the category of equations studied in ref. [23], and numerical experiments reported in Section 3 are indeed in qualitative agreement with those in that reference. The reason for the degeneracy at the other Hamiltonian-Hopf point is described by a mathematical result stated in Proposition 1. At this point the system has a two-dimensional invariant subspace located in the zero energy surface, and this degeneracy is inherited by the normal form. The invariant subspace contains a non-zero equilibrium connected to itself by a homoclinic orbit, and numerically a branch of such equilibria is found to emanate from the degenerate Hamiltonian-Hopf point. Since both equilibria lie in the zero energy surface there is also the possibility of heteroclinic connections between them (corresponding to *kink* or front solutions of the original system of PDEs). Numerical experiments confirm the presence of two such kink solutions along the branch, which acts as a barrier between parts of parameter space associated with sub- and supercritical behaviour: solitary waves on branches passing between the two regions interact globally with the kinks (see Section 3).

In this Letter we focus exclusively on *primary* homoclinic solutions, namely those which bifurcate from zero at the Hamiltonian-Hopf points. This study includes the solutions into which the primary solutions evolve along a continuous branch. However, it should be remarked that there are necessarily infinitely many other geometrically distinct homoclinic orbits to (7), (8) in a neighbourhood of a subcritical Hamiltonian-Hopf bifurcation that are not described by the normal-form theory itself. These orbits, as established by rigorous variational methods [4], are generically *multi-bumped* solutions that resemble 'bound states' consisting of multiple copies of the bifurcating solutions. Approximate methods for several distinct systems [24, 3] show that such solutions lie on branches that never reach the Hamiltonian-Hopf point: each branch turns at a limit point and the sequence of limit points accumulates at the Hamiltonian-Hopf point. Note also that other bifurcation mechanisms may give rise to homoclinic solutions in other parts of parameter space, but such solutions will not be examined here.

2 Normal-form analysis

The first step in the normal-form analysis of (7), (8) is to examine the corresponding linearized system. Its eigenvalues λ satisfy the equation

$$\lambda^4 + (\eta - 2c)\lambda^2 + c^2 - c\eta - s = 0, \tag{10}$$

the discriminant of which vanishes when $\eta^2 + 4s = 0$, so that repeated eigenvalues (corresponding to *Hamiltonian-Hopf bifurcations* if imaginary or *node-focus transitions* if real) occur when $s = -1$ and $\eta = \pm 2$. Hamiltonian-Hopf bifurcations occur for $c < \eta/2$ and node-focus transitions for $c > \eta/2$; at $c = \eta/2$ there is a zero eigenvalue of multiplicity four. A double zero eigenvalue occurs whenever $c^2 - c\eta - s = 0$, so that

$$c = \frac{\eta}{2} \pm \frac{(\eta^2 + 4s)^{\frac{1}{2}}}{2};$$

the positive sign gives a *pitchfork bifurcation* and the negative sign a *degenerate saddle-centre bifurcation*. Figure 1 summarizes these conclusions for $s = -1$, the case of interest here since it admits a Hamiltonian-Hopf bifurcation.

Let us now concentrate on the Hamiltonian-Hopf bifurcation at $s = -1$, $\eta = 2$, $c < 1$ and introduce the bifurcation parameter $\alpha = \eta - 2$. According to the transformation theory given in [10, 22], equations (7), (8) can be transformed into the new Hamiltonian system

$$\dot{A} = \frac{\partial H}{\partial \bar{B}}, \qquad \dot{B} = -\frac{\partial H}{\partial \bar{A}}, \tag{11}$$

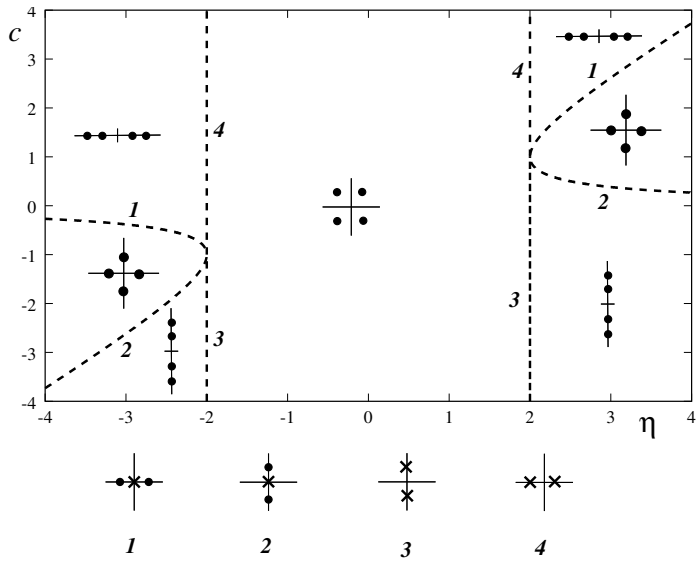

Figure 1: The eigenvalues of (7), (8) for $s = -1$; the numbered curves show the location of pitchfork, degenerate saddle-centre, Hamiltonian-Hopf and node-focus bifurcations respectively.

where

$$H = \mathrm{i}\omega(A\bar{B} - \bar{A}B) + |B|^2 + H_{\mathrm{NF}}(|A|^2, \mathrm{i}(A\bar{B} - \bar{A}B), \alpha) + R(A, B, \alpha), \tag{12}$$

A, B are complex coordinates, $\pm\mathrm{i}\omega$ are the double eigenvalues at $\alpha = 0$, H_{NF} is a real polynomial function of its first two arguments with coefficients which depend analytically upon α and R is a higher-order remainder term. In these coordinates the reversibility is represented by the invariance of (11) under the transformation $(z, A, B) \mapsto (-z, \bar{A}, -\bar{B})$. We refer to the system obtained by omitting the remainder term in (12) as the *normal form* for (7), (8). This normal form is completely integrable (the quantities H and $K = \frac{\mathrm{i}}{2}(A\bar{B} - \bar{A}B)$ are independent first integrals) and has been studied in detail by Iooss & Pérouéme [18]. They showed that along orbits in the surface $\{H = K = 0\}$ (upon which homoclinic orbits lie) the quantity $x = |A|^2$ satisfies the equation

$$\left(\frac{\mathrm{d}x}{\mathrm{d}z}\right)^2 = 4f(x), \qquad f(x) = -xH_{\mathrm{NF}}(x, 0, \alpha), \tag{13}$$

and periodic orbits correspond to double zeros of $f(x)$. Information about the existence of homoclinic orbits may then be obtained from the graph of $f(x)$ in an elementary fashion by regarding equation (13) as the law of conservation of zero total energy for a particle with unit mass and position x moving in a potential $-4f(x)$.

Write

$$H_{\mathrm{NF}}(x, 0, \alpha) = q_1\alpha x - \frac{1}{2}q_2x^2 - \frac{1}{3}q_4x^3 + \ldots, \tag{14}$$

where $q_1 > 0$, so that Hamilton's equations are hyperbolic for $\alpha < 0$. Iooss & Pérouème demonstrate by a scaling argument that generically it suffices to approximate $f(x)$ by a cubic polynomial; they distinguish between *subcritical* and *supercritical* codimension-one behaviour via the sign of the coefficient q_2. For $q_2 < 0$ a circle of small-amplitude homoclinic orbits bifurcate from zero at $\alpha = 0$ into negative α, two of which are reversible and survive the introduction of the remainder term R in (12). The orbits consist of harmonic waves modulated by a slowly decaying exponential envelope (e.g. see the bottom right inset in Figure 2 below); the two reversible solutions differ in phase by π. On the other hand no homoclinic bifurcation takes place for $q_2 > 0$. When q_2 is small it is necessary to use a different scaling and to retain the

quartic terms in $f(x)$; a complete unfolding of this codimension-two situation can be obtained using q_2 and α as independent small parameters [7, 23]. For $q_4 > 0$ a subcritical bifurcation of homoclinic orbits from zero occurs at $\alpha = 0$, $q_2 < 0$. These homoclinic orbits disappear as α is decreased from zero to

$$\alpha = -\frac{3q_2^2}{16q_1q_4} \tag{15}$$

by colliding with a periodic orbit and forming a heteroclinic connection between the zero equilibrium and the periodic orbit [23, Fig. 2]. A heuristic argument given in ref. [23, §5] shows that introduction of the remainder term R generically causes a heteroclinic connection to persist in a small region of parameter space around the critical curve (15) and to be approached by 'snaking' branches of homoclinic orbits (see Figure 5 below). For $q_4 < 0$ homoclinic bifurcation again takes place for $\alpha = 0$, $q_2 < 0$, but now the homoclinic solutions exist for all negative values of α and can be followed up to $\alpha = 0$, $q_2 > 0$, where they decay algebraically rather than exponentially [23, Fig. 3]. It is known that the two reversible homoclinic orbits with algebraically decaying tails also survive the introduction of the remainder term R [17].

Let us now carry out the above normal-form analysis for the Hamiltonian-Hopf bifurcation that occurs in (7), (8) at $s = -1$, $\eta = 2$, $c < 1$. The vector

$$e = \left(\frac{1}{2\sqrt{1-c}}, \frac{\mathrm{i}}{2}, -\frac{1}{2\sqrt{1-c}}, \frac{\mathrm{i}}{2}\right),$$

is an eigenvector of the linearized system corresponding to the eigenvalue $\mathrm{i}\sqrt{1-c}$ and

$$f = \left(\frac{\mathrm{i}(-3+2c)}{4(1-c)}, \frac{1-2c}{4\sqrt{1-c}}, \frac{\mathrm{i}(-1+2c)}{4(1-c)}, \frac{-3+2c}{4\sqrt{1-c}}\right)$$

is a generalised eigenvector; their counterparts for the eigenvalue $-\mathrm{i}\sqrt{1-c}$ are therefore $\bar{e}$ and $\bar{f}$. These vectors have been chosen so that $\{e, f, \bar{e}, \bar{f}\}$ is a symplectic basis with respect to the canonical symplectic 2-form associated with (9). It follows that

$$(q_1, p_1, q_2, p_2) = Ae + Bf + \bar{A}\bar{e} + \bar{B}\bar{f}, \qquad A, B \in \mathbb{C},$$

defines a change of variable which transforms (7), (8) into the form (11) with

$$\begin{aligned} H &= H_{\mathrm{KdV}}(q_1, q_2, p_1, p_2) \\ &= \mathrm{i}\sqrt{1-c}(A\bar{B} - \bar{A}B) + |B|^2 + \frac{\alpha}{2}\left(-\frac{1}{2\sqrt{1-c}}(A+\bar{A}) + \frac{(-1+2c)\mathrm{i}}{4(1-c)}(B-\bar{B})\right)^2 \\ &\quad + \left(\frac{1}{2\sqrt{1-c}}(A+\bar{A}) + \frac{(-3+2c)\mathrm{i}}{4(1-c)}(B-\bar{B})\right)^3 \\ &\quad - \frac{\mu}{3}\left(-\frac{1}{2\sqrt{1-c}}(A+\bar{A}) + \frac{(-1+2c)\mathrm{i}}{4(1-c)}(B-\bar{B})\right)^3, \end{aligned} \tag{16}$$

and Hamilton's equations are given explicitly by the formulae

$$\begin{aligned} \dot{A} &= \mathrm{i}\sqrt{1-c}\,A + B + \frac{(2c-1)\alpha\mathrm{i}}{4(1-c)}\left(-\frac{1}{2\sqrt{1-c}}(A+\bar{A}) + \frac{(-1+2c)\mathrm{i}}{4(1-c)}(B-\bar{B})\right) \\ &\quad + \frac{3(2c-3)\mathrm{i}}{4(1-c)}\left(\frac{1}{2\sqrt{1-c}}(A+\bar{A}) + \frac{(-3+2c)\mathrm{i}}{4(1-c)}(B-\bar{B})\right)^2 \\ &\quad + \frac{\mu(-1+2c)\mathrm{i}}{4(1-c)}\left(-\frac{1}{2\sqrt{1-c}}(A+\bar{A}) + \frac{(-1+2c)\mathrm{i}}{4(1-c)}(B-\bar{B})\right)^2, \end{aligned} \tag{17}$$

$$\dot{B} = \mathrm{i}\sqrt{1-c}\,B + \frac{\alpha}{4\sqrt{1-c}}\left(-\frac{1}{2\sqrt{1-c}}(A+\bar{A}) + \frac{(-1+2c)\mathrm{i}}{4(1-c)}(B-\bar{B})\right)$$

$$
\begin{aligned}
&- \frac{3}{2\sqrt{1-c}}\left(\frac{1}{2\sqrt{1-c}}(A+\bar{A}) + \frac{(-3+2c)\mathrm{i}}{4(1-c)}(B-\bar{B})\right)^2 \\
&- \frac{\mu}{2\sqrt{1-c}}\left(-\frac{1}{2\sqrt{1-c}}(A+\bar{A}) + \frac{(-1+2c)\mathrm{i}}{4(1-c)}(B-\bar{B})\right)^2 . \qquad (18)
\end{aligned}
$$

The Hamiltonian (16) can be transformed into the form (12) using a sequence of near identity canonical transformations, and standard methods in normal-form theory show that the coefficients in equation (14) are

$$
\begin{aligned}
q_1 &= \frac{1}{4(1-c)}, \\
q_2 &= \frac{-(3+\mu)(102+15c(-3+\mu)+4\mu)}{18(1-c)^3}, \\
q_4 &= \frac{1}{20736(1-c)^8}\Big(-3600c^4(\mu^2-9)^2 + 24c^3(9-\mu^2)(12267+\mu(2040+163\mu)) \\
&\qquad -4(3+\mu)(1293921+\mu(445527+28\mu(1332+25\mu))) \\
&\qquad -12c(3+\mu)(-558441+\mu(-42750+\mu(20829+1162\mu))) \\
&\qquad -9c^2(3+\mu)(383697+\mu(-26955+\mu(-5001+2003\mu)))\Big).
\end{aligned}
$$

Observe that q_2 vanishes at $\mu=-3$ and at $\mu=\mu_0=3(-34+15c)/(15c+4)$. Clearly $\mu_0<-3$ for $-4/15<c<1$ (e.g.$\mu_0=-42/5$ for $c=2/5$, the case investigated numerically in Section 3 below) with $\mu_0\to-\infty$ as $c\downarrow -4/15$; on the other hand $\mu_0>-3$ for $c<-4/15$ with $\mu_0\to+\infty$ as $c\uparrow -4/15$. The coefficient q_2 is however always positive in the interval between -3 and μ_0 (the supercritical case) and negative outside this interval (the subcritical case). Note also that

$$
\begin{aligned}
q_4|_{\mu=-3} &= 0, \\
q_4|_{\mu=\mu_0} &= \frac{405(7072+15675c(2-c))}{(1-c)^4(4+15c)^4} > 0,
\end{aligned}
$$

so that the degenerate Hamiltonian-Hopf point at $\eta=2$, $\mu=\mu_0$ falls into the category studied in [23]. The fact that $q_4|_{\mu=-3}=0$ is a consequence of the following mathematical result, whose proof is established by a careful examination of the sequence of coordinate changes which transforms the Hamiltonian into its form (12); it is a particular instance of the observation that in general normal-form transformations preserve symmetries and invariances.

Proposition 1 *Consider the reversible Hamiltonian system*

$$
\begin{aligned}
\dot{A} &= \mathrm{i}\omega A + B + f(\alpha, A, B, \bar{A}, \bar{B}), \\
\dot{B} &= \mathrm{i}\omega B + g(\alpha, A, B, \bar{A}, \bar{B}),
\end{aligned}
$$

in which f and g are real functions of their arguments of order $|(\alpha,A,B)||(A,B)|$ (so that a Hamiltonian-Hopf bifurcation takes place at $\alpha=0$). Suppose that $g(0,A,0,\bar{A},0)$ is identically zero, so that $\{B=0\}$ is an invariant subspace when $\alpha=0$. The normal-form transformations preserve this degeneracy; in particular $H_{\mathrm{NF}}(x,0,0)=0$ in the above notation and $\{B=0\}$ is an invariant subspace for the normal form when $\alpha=0$.

An examination of equations (17), (18) shows that the condition in Proposition 1 is satisfied precisely when $\mu=-3$, so that the system has a two-dimensional invariant subspace $\{B=0\}$ at the degenerate Hamiltonian-Hopf point $(\eta,\mu)=(2,-3)$. This invariant subspace is given by $\{v=-u\}$ in the original coordinates, and it is readily confirmed that it lies in the zero energy surface. The flow in the invariant subspace is described by the system

$$
\ddot{u} = cu - u + 3u^2, \qquad v=-u,
$$

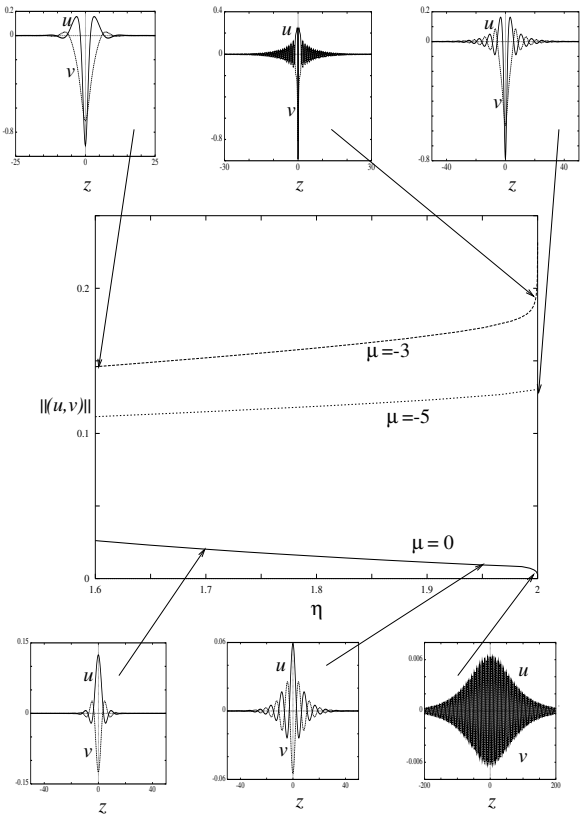

Figure 2: Branches of primary homoclinic solutions to (7), (8) for $s = -1$, $c = 0.4$ which approach the Hamiltonian-Hopf point at $\eta = 2$ for three different values of μ. The ordinate $\|(u, v)\|$ in this and subsequent bifurcation diagrams is a scaling of the vector L^2-norm of (u, u', v, v').

which can be solved by elementary methods. One finds that it contains the non-zero equilibrium point

$$(u, v) = \left(\frac{1-c}{3}, \frac{c-1}{3}\right), \tag{19}$$

which is connected to itself by the homoclinic orbit

$$u = \frac{1-c}{3} + \frac{1-c}{6}\mathrm{sech}^2\left(\frac{\sqrt{1-c}\,z}{2}\right), \qquad v = \frac{c-1}{3} + \frac{c-1}{6}\mathrm{sech}^2\left(\frac{\sqrt{1-c}\,z}{2}\right).$$

A straightfoward application of the implicit function theorem shows that a branch $(u^\star, v^\star, \mu^\star) = (u^\star(\eta), v^\star(\eta), \mu^\star(\eta))$ of non-zero equilibrium solutions of (17), (18) lying in its zero energy surface emanates from the Hamiltonian-Hopf point $\eta = 2$, $\mu = -3$. An explicit calculation shows that the equilibrium $(u^\star(2), v^\star(2))$ at $\mu = \mu^\star(2) = -3$ is hyperbolic, and one would therefore expect its homoclinic connection to persist along the branch. There is also the possibility of heteroclinic connections between the zero and nonzero equilibria (kinks). These matters are explored in detail in the numerical results that follow, which confirm that a homoclinic connection to $(u^\star(\eta), v^\star(\eta))$ exists at each point of the curve $\mu = \mu^\star(\eta)$ together with two heteroclinic connections between 0 and $(u^\star(\eta), v^\star(\eta))$.

3 Numerical results

This section presents the conclusions of a numerical investigation inspired by the above normal-form theory. We concentrate upon the 'primary' homoclinic orbits that are created by a

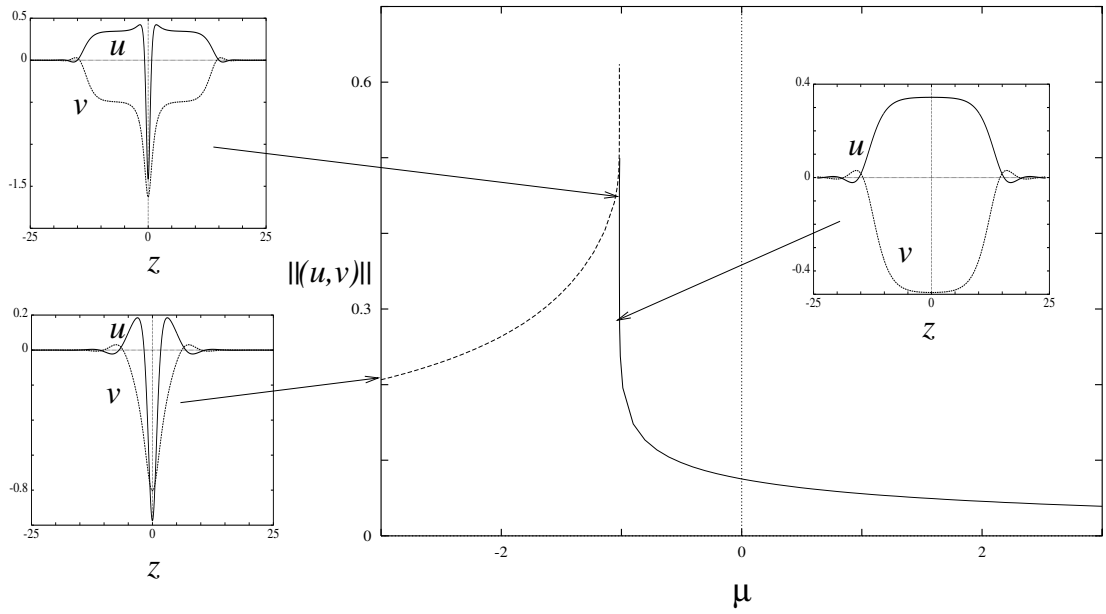

Figure 3: Continuation in μ of two distinct homoclinic solutions to (7), (8) for $s = -1$, $c = 0.4$ and $\eta = 1.6$, towards a kink solution at $\mu \approx -1.02$.

Hamiltonian-Hopf bifurcation at $\eta = 2$, $c < 1$; for these orbits we have performed a range of path-following experiments in the parameters η and μ using the homoclinic continuation part of the software AUTO [9]. The parameter c will henceforth be fixed at the illustrative value $2/5$ since the numerics show that the behaviour of solutions at this value is typical for values of c in the range $(-4/15, 1)$ for which $\mu_0 < -3$. The above normal-form theory therefore predicts a subcritical bifurcation of two small-amplitude reversible homoclinic orbits at $\eta = 2$ for $\mu < \mu_0$ and $\mu > -3$.

3.1 The degenerate Hamiltonian-Hopf point at $\mu = -3$

Figure 2 shows numerical computations of branches of homoclinic solutions near $\eta = 2$ for three different values of μ. The curve for $\mu = 0$ shows behaviour typical of a subcritical bifurcation from the Hamiltonian-Hopf point at $\eta = 2$ and is indicative of the behaviour for all $\mu > -3$: as η approaches 2 the amplitude of the solitary wave decreases to zero, and during this process the core of the wave spreads out so that more and more large-scale oscillations become visible. Note that the solution along this branch is a solitary wave of elevation in the u-component (having a positive maximum at $z = 0$) and of depression for the v-component (having a central negative minimum).

The normal-form analysis predicts no such subcritical bifurcation for $\mu < -3$, since then $q_2 > 0$. This prediction is indeed confirmed by the numerics. Consider, for example, the branch in Figure 2 with $\mu = -5$. Here the L^2-norm of the solution remains finite as η approaches 2 and the central disturbance does not decay to zero. It follows that this branch, despite its existence right up $\eta = 2$ (where its solitary-wave tails decay algebraically rather than exponentially) *does not bifurcate from zero at* $\eta = 2$, and hence is not captured by the normal-form analysis for a Hamiltonian-Hopf bifurcation. Furthermore, as is clear from the insets in Figure 2, solutions along the branch with $\mu = -5$ are qualitatively different to those on the $\mu = 0$ branch; they are now such that both u- and v-components are waves of depression. It is therefore clear that these two branches cannot be smoothly continued into each other, and there must some global bifurcation that causes the transition between these branches at $\mu = 0$ and $\mu = -5$.

The transition between these two types of behaviour occurs at $\mu = -3$, yet Figure 2 shows

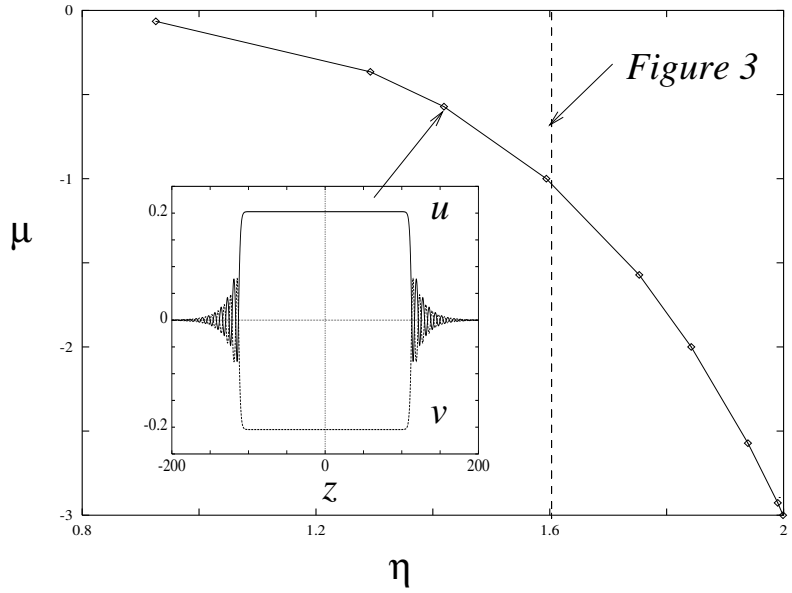

Figure 4: Two-parameter continuation in the (η, μ)-plane of kink solutions to (7), (8) with $s = -1$ and $c = 0.4$.

that the corresponding branch for this critical μ-value is qualitatively similar to that for $\mu = -5$. Figures 3 and 4 shed more light on this matter: the global bifurcation that causes the transition between the 'depression-elevation' and 'pure depression' solitary waves occurs as both approach a pair of heteroclinic connections to the non-zero equilibrium point found in Section 2. Figure 3 depicts the results of numerical continuation in μ for η fixed at a value slightly less than 2 (the Hamiltonian-Hopf point). Note the spike at $\mu = \mu^\star \approx -1.02$; the 'pure depression' and 'depression-elevation' solitary waves are respectively to the left and right of this spike. Taking the solution branch on the right, one finds that it reaches a critical state as $\mu \downarrow \mu^\star$. Here the solution has infinite L^2-norm as it develops into a pair of heteroclinic connections (kinks) between the zero equilibrium and the nonzero equilibrium at $(u, v) = (u^\star, v^\star) \approx (0.34, -0.49)$. The solution on the branch to the left develops into a pair of kinks and a homoclinic connection to $(u^\star, v^\star)$ as $\mu \uparrow \mu^\star$. Numerically the branch has been truncated in the Figure 3, but its infinite slope at $\mu = \mu^\star$ is apparent, as is the form of solutions shown in the insets which depict the profiles of the homoclinic solutions on either side of the transition. To the right the solutions resemble a concatenation of a heteroclinic orbit connecting 0 at $z = -\infty$ to $(u^\star, v^\star)$ at $z = +\infty$ and a heteroclinic orbit connecting $(u^\star, v^\star)$ at $z = -\infty$ to 0 at $z = +\infty$; to the right the solutions take the same form with a homoclinic connection to $(u^\star, v^\star)$ sandwiched in the middle.

Figure 4 shows the branch $\mu = \mu^\star(\eta)$ of non-zero equilibria $(u^\star, v^\star)$ found in Section 2 along which the numerics indicate the presence of two heteroclinic connections between 0 and $(u^\star, v^\star)$ and a homoclinic connection to $(u^\star, v^\star)$. Recall that this branch terminates at the degenerate Hamiltonian-Hopf point $(\eta, \mu) = (2, -3)$. Reversible homoclinic solutions are created at a subcritical Hamiltonian-Hopf bifurcation for $\mu > -3$, $\eta = 2$ and can be followed to the curve $\mu = \mu^\star(\eta)$, where they undergo the qualitative change described above. Below the curve $\mu = \mu^\star(\eta)$ they can be followed to $\eta = -2$, $\mu < -3$, where they have finite amplitude.

3.2 The degenerate Hamiltonian-Hopf point at $\mu = \mu_0$

Let us now examine the other parameter interval where the normal-form analysis gives a subcritical Hamiltonian-Hopf bifurcation, namely $\mu < \mu_0$.

Figure 5 shows a bifurcation at $\mu = -13.35$ of the two reversible homoclinic orbits that

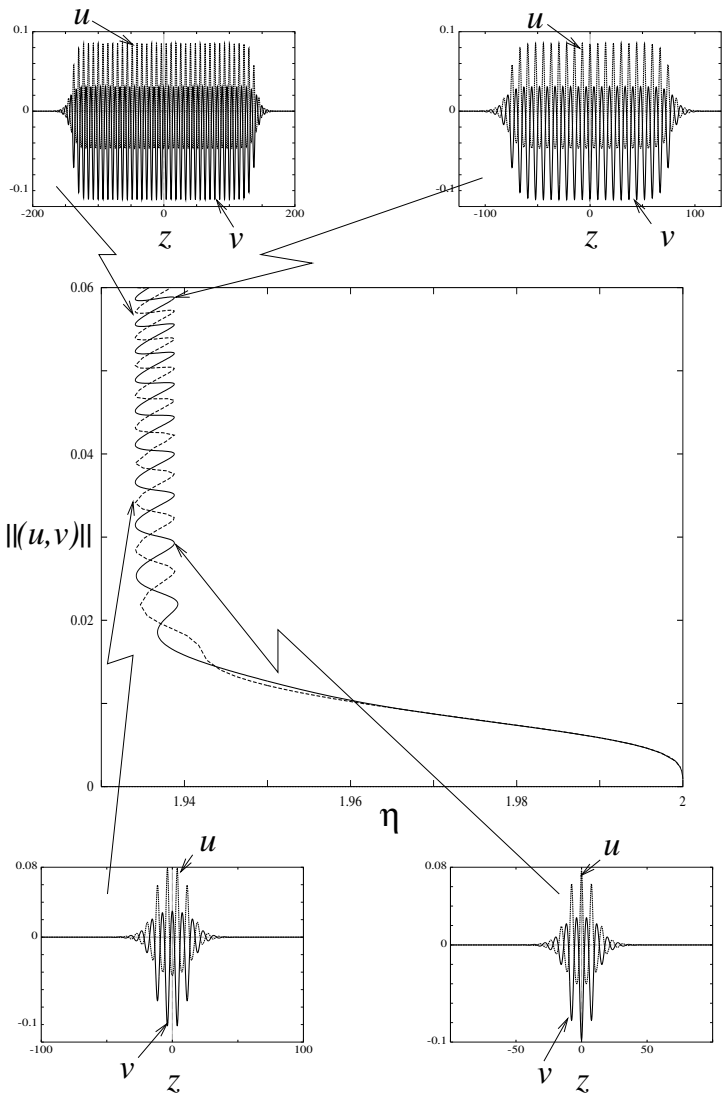

Figure 5: Continuation in η of the two bifurcating primary homoclinic solutions to (7), (8) with $s = -1$, $c = 0.4$ and $\mu = -13.35$, showing the disappearance of the homoclinic solutions for η close to 2 via a 'snaking' bifurcation diagram. Note from the insets that the homoclinic solutions develop long periodic cores with the u-component having a positive mean and the v-component a negative mean.

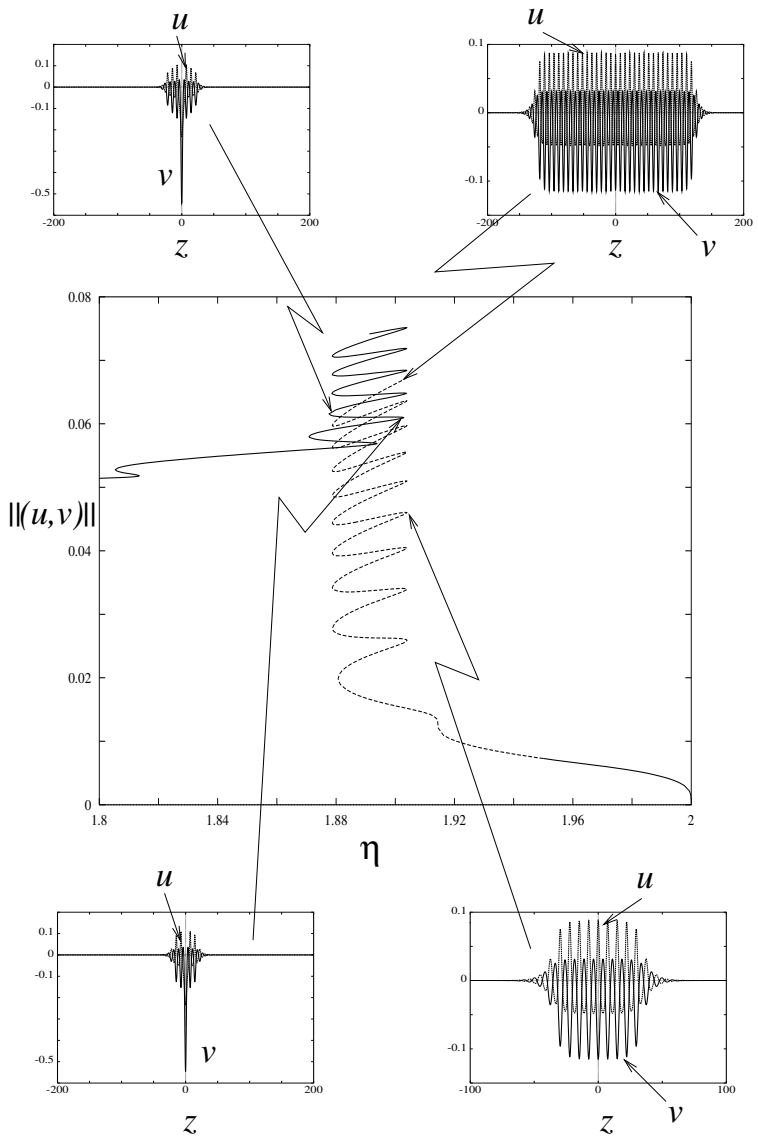

Figure 6: As in Figure 5 for η close to 2, but for $\mu = -15.35$ and now showing a new 'supercritical' solution (solid line) in comparison with one of the primary solutions (dashed line).

originate from the Hamiltonian-Hopf point at $\eta = 2$. The bifurcation diagram shows how the branches 'snake' back and forth, the solution gaining an extra pair of 'bumps' close to a periodic solution as it traverses between each successive pair of limit points. In this fashion a homoclinic solution with arbitrary large norm and arbitrarily many finite-amplitude bumps is created. The successive limit points converge rapidly to two distinct η-values. Notice how the bifurcation branches become intertwined and their limit points converge to the same two η-values. The first branch creates solutions with odd numbers of bumps close to a periodic orbit while the second creates homoclinic solutions with an even number of bumps close to the same periodic orbit. In this periodic solution the variables u and v have respectively a negative and a positive mean.

These numerical results are in complete accordance with the heuristic explanation and numerical results presented for different systems in refs. [23, 15]. The premise in that work was that these structures should emerge in an unfolding of the heteroclinic connection between the zero equilibrium and a periodic orbit predicted by the Hamiltonian-Hopf normal-form analysis for $-1 \ll q_2 < 0$ and $q_4 > 0$. In Section 2 it was shown that this situation arises in the present context at the degenerate Hamiltonian-Hopf point $\eta = 2$, $\mu = \mu_0$.

The situation for our coupled KdV system is, however, more complicated. Not only do

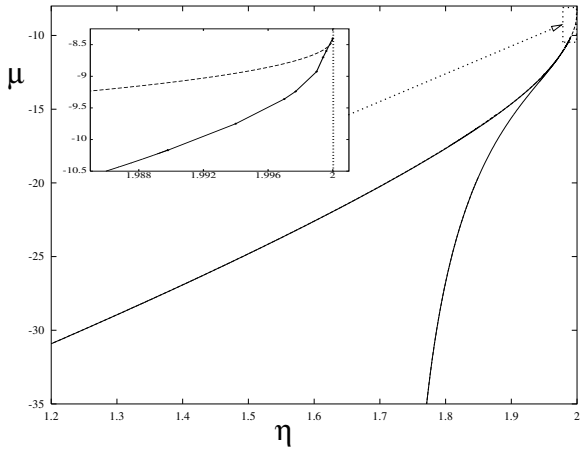

Figure 7: Two-parameter continuation in η and μ of the left and right-hand limit points of large norm in Figures 5 and 6. The inset shows the curves near $\eta = 2$ which at the scale depicted contract onto the single solid line (connecting data points which were calculated indirectly via continuation in η only). The dashed line in the inset represents the formula (15) evaluated using the normal-form coefficients at $\mu = \mu_0$.

the branches of primary homoclinic orbits terminate in a 'snake', but so do a pair of branches of larger-amplitude homoclinic solutions that approach from smaller values of η. For reasons that will become apparent we shall refer to these now solutions as 'supercritical'. Figure 6 depicts a branch of one of these new solutions and compares it with one of the primaries. This branch also snakes, creating a homoclinic solution with arbitrary large norm and arbitrarily many large-amplitude bumps. The successive limit points converge rapidly to the *same* two η-values as the primary snaking branches. It would appear that supercritical homoclinic solutions form a continuous branch with those homoclinic orbits that exist for $\mu^\star < \mu < \mu_0$ (see above). Recall that these solutions can be continued up to the *supercritical* Hamiltonian-Hopf point at $\eta = 2$, $-3 < \mu < \mu_0$ (hence the name), and of course via the global bifurcation along the curve $\mu = \mu^\star(\eta)$ to a subcritical bifurcation at $\eta = 2$, $\mu < -3$.

Note that Figures 5 and 6 are plotted for different μ-values. In fact the picture remains qualitatively valid over a large range of $\mu < \mu_0$. As μ is decreased the width of the snake widens and its centre moves way from $\eta = 2$. Conversely, as $\mu \uparrow \mu_0$, the whole structure shrinks into a neighbourhood of the degenerate Hamiltonian-Hopf bifurcation at $\eta = 2$. Figure 7 shows how the left and right limit points of the snaking primary branch vary with η and μ. These curves were computed by tracing the limit points of the branch for homoclinic orbits with sufficiently large norm. Similar curves computed for the supercritical solutions appear numerically to be identical with those for the primaries. Note how the width of the snake becomes very thin as the curves approach the degenerate Hamiltonian-Hopf point at $(\eta, \mu) = (2, \mu_0)$. Analytical evidence to be presented elsewhere suggests that the width of the snake is an exponentially small function of $\mu - \mu_0$. The inset in Figure 7 shows a comparison between the limit points on the snake and the expression (15) where the normal form predicts a heteroclinic connection between the origin and a periodic orbit. Note that the normal-form prediction, which only gives the quadratic part of the curve, is at best only valid for a tiny range of η-values just less than 2.

4 Conclusion

In summary, this Letter has demonstrated how gap solitary waves in coupled systems of wave equations may be generated and destroyed in the neighbourhood of degenerate Hamiltonian-Hopf bifurcation points. Specifically, via scaling we have reduced a class of systems which includes

models derived from different physical applications to the analysis of a three-parameter system of coupled second-order equations. For such a system we have identified two degeneracies in the normal form of the Hamiltonian-Hopf bifurcation which occurs for $\eta = 2$; at $\mu = \mu_0$ and at $\mu = -3$. The normal-form unfolding of the former shows agreement with the analysis and numerical results for a higher-order KdV equation in ref. [23]: there is a delicate 'snaking' back and forth in a bifurcation diagram of a pair of intertwined branches of solitary waves. The bifurcation at $\mu = -3$ is entirely new and Proposition 1 above explains why it occurs for systems of this type. Moreover, we have shown how this bifurcation leads to the creation of kink solutions which play an organizing role in bounding parameter regions containing qualitatively distinct solitary waves. Finally, our numerical results indicate how these small amplitude solutions involved with the two degeneracies fit together globally in the (η, μ)-parameter plane.

An important feature not discussed in this Letter is the question of PDE stability of the new solitary-wave solutions. This question is not straightforward since the equations are in general nonintegrable. Any investigation is left for future work, but it is worth remarking that there is analytical and numerical evidence available for various fifth-order KdV models [21, 5, 8] which suggest that some of the more complex solitary-wave solutions akin to those found here may indeed be stable.

References

[1] T. B. Benjamin. Impulse, flow-force and variational principles. *IMA J. Appl. Math.*, 32:3–68, 1984.

[2] J. L. Bona, G. Ponce, J.-C. Saut, and M. M. Tom. A model system for strong interaction between internal solitary waves. *Comm. Math. Phys.*, 143:287–313, 1992.

[3] B. Buffoni, A. R. Champneys, and J. F. Toland. Bifurcation and coalescence of a plethora of homoclinic orbits for a Hamiltonian system. *J. Dyn. Diff. Eqns.*, 8:221–281, 1996.

[4] B. Buffoni and M. D. Groves. A multiplicity result for solitary gravity-capiliary water waves via critical-point theory. *Arch. Rat. Mech. Anal.*, 146:183–220, 1999.

[5] A. V. Buryak and A. R. Champneys. On the stability of solitary wave solutions of the 5th-order KdV equation. *Phys. Lett. A*, 233:58–62, 1997.

[6] A. R. Champneys and M. D. Groves. A global investigation of solitary-wave solutions to a two-parameter model for water waves. *J. Fluid Mech.*, 342:199–229, 1997.

[7] F. Dias and G. Iooss. Capillary-gravity interfacial waves in infinite depth. *Europ. J. Mech. B/Fluids*, 15(3):367–393, 1996.

[8] F. Dias and E. A. Kuznetsov. Nonlinear stability of solitons in the fifth-order Korteweg-De Vries equation. *Phys. Lett. A*, 263:98–104, 1999.

[9] E. J. Doedel, A. R. Champneys, T. R. Fairgrieve, Yu. A. Kuznetsov, B. Sandstede, and X. J. Wang. AUTO97 continuation and bifurcation software for ordinary differential equations, 1997. Technical Report, Concordia University. Software available by anonymous ftp from `ftp.cs.concordia.ca`, directory `pub/doedel/auto`.

[10] C. Elphick, E. Tirapegui, M. E. Brachet, P. Coullet, and G. Iooss. A simple global characterization for normal forms of singular vector fields. *Physica D*, 29:95–127, 1987.

[11] G. Gottwald, R. Grimshaw, and B. Malomed. Parametric envelope solitons in coupled Korteweg-de Vries equations. *Phys. Lett. A*, 227:47–54, 1997.

[12] R. Grimshaw and J. Gear. Weak and strong interactions between internal solitary waves. *Stud. Appl. Math.*, 70:235–258, 1984.

[13] R. Grimshaw, B. Malomed, and E. Benilov. Solitary waves with damped oscillatory tails: an analysis of the fifth-order Korteweg-de Vries equation. *Physica D*, 77:473–485, 1994.

[14] R. Grimshaw and B. A. Malomed. New type of gap soliton in a coupled Korteweg-de Vries wave system. *Phys. Rev. Lett.*, 72(7):949–953, 1994.

[15] G. W. Hunt, M. A. Peletier, A. R. Champneys, P. D. Woods, M. A. Wadee, C. J. Budd, and G. J Lord. Cellular buckling in long structures, 1999. In press with *Nonlinear Dynamics.*

[16] J. K. Hunter and J. Scheurle. Existence of perturbed solitary wave solutions to a model equation for water-waves. *Physica D*, 32:253–268, 1988.

[17] G. Iooss. Existence d'orbites homoclines á un équilibre elliptique pour un système réversible. *C. R. Acad. Sci. Paris, Ser. 1*, 324:993–997, 1997.

[18] G. Iooss and M. C. Pérouème. Perturbed homoclinic solutions in reversible 1:1 resonance vector fields. *J. Diff. Eqns.*, 102:62–88, 1993.

[19] T. Kakutani and H. Ono. Weak non-linear hydromagnetic waves in cold collisionless plasma. *J. Phys. Soc. Japan*, 26:1305–219, 1969.

[20] T. Kawahara. Oscillatory solitary waves in dispersive media. *J. Phys. Soc. Japan*, 33:260–264, 1972.

[21] S. P. Levandosky. A stability analysis of fifth-order water wave models. *Physica D*, 125:222–240, 1999.

[22] K. R. Meyer and G. R. Hall. *Introduction to Hamiltonian dynamical systems and the N-body problem.* Springer-Verlag, 1992.

[23] P. D. Woods and A. R. Champneys. Heteroclinic tangles in the unfolding of a degenerate Hamiltonian-Hopf bifurcation. *Physica D*, 129:147–170, 1999.

[24] T. S. Yang and T. R. Akylas. On asymmetric gravity-capillary solitary waves. *J. Fluid Mech*, 330:215–232, 1997.

[25] J. A. Zufiria. Symmetry breaking in periodic and solitary gravity-capillary waves on water of finite depth. *J. Fluid Mech.*, 184:183–206, 1987.